

Partition function zeros of adsorbing Dyck paths

N.R. Beaton¹†

¹School of Mathematics and Statistics, The University of Melbourne, VIC 3010, Australia

E.J. Janse van Rensburg²‡

²Department of Mathematics and Statistics, York University, Toronto, Ontario M3J 1P3, Canada

Abstract. The zeros of the size- n partition functions for a statistical mechanical model can be used to help understand the critical behaviour of the model as $n \rightarrow \infty$. Here we use weighted Dyck paths as a simple model of two-dimensional polymer adsorption, and study the behaviour of the partition function zeros, particularly in the thermodynamic limit. The exact solvability of the model allows for a precise calculation of the locus of the zeros and the way in which an edge-singularity on the positive real axis is formed.

PACS numbers: 02.10.Ox, 05.50.+q, 64.60.Cn, 65.40.G-, 68.43.Mn

AMS classification scheme numbers: 05A15, 82B41, 82B23

† nrbeaton@unimelb.edu.au

‡ rensburg@yorku.ca

1. Introduction

Lee-Yang [20, 25] and Fisher zeros [6, 7] have been examined as a mathematical mechanism whereby critical points appear in the thermodynamic limit in models in statistical mechanics. The Lee-Yang theorem (see, for example, theorem 5.1.2 in reference [22]) shows that Lee-Yang zeros accumulate on the unit circle in the complex plane in a broad class of lattice models in statistical mechanics, including the lattice gas and Ising model. Studies of Lee-Yang zeros include the the Potts model [17, 18], lattice ϕ^3 theories [19] and the n -vector model [3].

In a finite size model with complex temperature or interaction strength, zeros in the partition function (the *Fisher zeros*) are (complex) non-analyticities in the free energy. In the thermodynamic limit these non-analyticities accumulate on a critical point on the positive real axis to form an *edge-singularity*. This mechanism is thought to be a mathematical mechanism whereby phase transitions arise in the thermodynamic limit in models of critical phenomena.

Partition function zeros in the complex temperature plane have a different distribution and do not generally accumulate on the unit circle. The distribution is generally dependent on the model, and is useful in modeling phase transitions [7]. In an Ising model with special boundary conditions the temperature plane zeros accumulate on two circles corresponding to the ferromagnetic and anti-ferromagnetic phases, a pattern which is not seen in the q -Potts model when $q > 2$ [17, 18].

In reference [15] the properties of partition and generating function zeros in a self-avoiding walk model of polymer adsorption were examined. While some generating function zeros were shown to accumulate on a circle in the complex plane, the partition function zeros appear to approach a limiting distribution which forms an edge-singularity at the critical adsorption point. In this paper our aim is to examine partition function zeros of adsorbing Dyck paths as a directed version of the adsorbing self-avoiding walk model in reference [15].

Adsorbing walks are models of the adsorption transition of a dilute polymer in a good solvent. The adsorption transition in a polymer is characterised by a conformational rearrangement of monomers, and by singular behaviour of thermodynamic quantities at the adsorption critical point (see for example references [4, 5, 10, 11]). The adsorbing self-avoiding walk is a standard model for linear polymer adsorption [8, 9, 23] and has been studied numerically in, for example, references [14, 16]. Exactly solvable models of directed lattice paths have also been used to model aspects of this transition [2, 12, 21, 24]. These directed models may be exactly solvable, and considerably more information can be obtained by analysing them. This may give some information on the adsorption critical point as the thermodynamic limit is taken in the more general case.

A *Dyck path* of length $2n$ is a walk on the square lattice \mathbb{Z}^2 , starting at $(0, 0)$ and ending at $(2n, 0)$, taking steps $(1, 1)$ and $(1, -1)$, and always remaining on or above the line $y = 0$ (see Figure 1). Let $d_{2n}(v)$ be the number of Dyck paths of length $2n$ which contain $v + 1$ vertices in the line $y = 0$ (these are called *visits*). We associate a weight a with each visit (excluding the first vertex) to obtain a partition function $D_{2n}(a)$, given

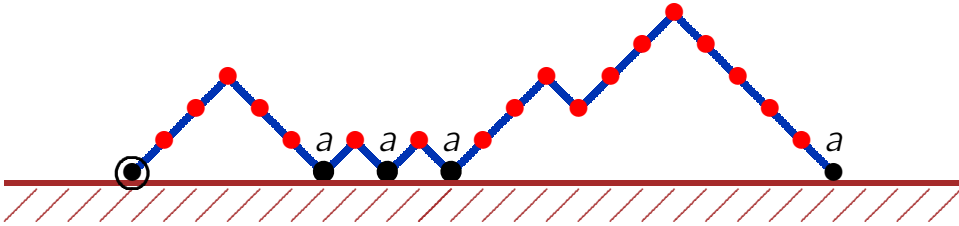


Figure 1: An adsorbing Dyck path of length 22. The path gives North-East and South-East steps in the positive square lattice (the x -axis is a hard wall) and is weighted by the number of returns (visits) to the wall (or adsorbing line), in this case a^4 . The path is conditioned to end in the adsorbing line.

by

$$D_{2n}(a) = \sum_v d_{2n}(v) a^v = \sum_{\ell=0}^n \frac{2\ell+1}{n+\ell+1} \binom{2n}{n+\ell} (a-1)^\ell, \quad (1)$$

see for example equation (5.32) in reference [13].

The partition function zeros a_ℓ of adsorbing Dyck paths of length $2n$ are the complex solutions of $D_{2n}(a) = 0$ in the a -plane. Since $D_{2n}(a)$ is a polynomial of degree n in a with non-negative coefficients, and the coefficient of a^n is equal to 1, the zeros a_ℓ occur as negative real numbers or as conjugate pairs, and $D_{2n}(a)$ factors as

$$D_{2n}(a) = \prod_{\ell=1}^n (a - a_\ell). \quad (2)$$

Since every non-empty Dyck path ends with a visit, $a = 0$ is a root of $D_{2n}(a)$ for all $n \geq 1$. We will henceforth refer to $a = 0$ as the *trivial zero*.

In Section 2 we examine the generating function of adsorbing Dyck paths in order to determine the asymptotic behaviour of $D_{2n}(a)$ for real and complex a , and find a “phase diagram” of sorts in the complex a -plane. In Section 3 we turn to the zeros of $D_{2n}(a)$, and show that they collect and are dense on the curve that separates the two phases in the a -plane. In Section 4 we use numerical techniques to estimate the locations of the zeros of $D_{2n}(a)$ for finite n . Finally in Section 5 we compute the exact asymptotics of the “leading” zero (the one with smallest positive argument), which approaches the critical point $a_c = 2$ as $n \rightarrow \infty$, this also being the location of a edge-singularity of the model.

2. The generating function of adsorbing Dyck paths and the complex a -plane

For a real and positive, the limiting free energy of adsorbing Dyck paths is given by

$$\mathcal{D}(a) = \lim_{n \rightarrow \infty} \frac{1}{2n} \log D_{2n}(a) = \begin{cases} \log 2 & \text{if } a \leq 2; \\ \log a - \frac{1}{2} \log(a-1) & \text{if } a \geq 2 \end{cases} \quad (3)$$

$\mathcal{D}(a)$ is singular at the point $a = 2$, corresponding to the adsorption phase transition. It is not immediately clear on how to generalise $\mathcal{D}(a)$ as a function of complex a .

The generating function of adsorbing Dyck paths is given by

$$D(t, a) = \sum_{n=0}^{\infty} D_{2n}(a) t^n = \frac{2}{2 - a(1 - \sqrt{1 - 4t})}. \quad (4)$$

It follows that $D(t, a)$ has one or two singularities in the t -plane, depending on the value of a : a square root singularity at $t = \frac{1}{4}$ for all $a \neq 0$ or 2, and a simple pole at $t = \frac{a-1}{a^2}$ when $|a-1| \geq 1$ and $a \neq 0$ or 2. When $a = 2$ these singularities coalesce and form a pole of order $\frac{1}{2}$. The *dominant* singularity (that is, the one closest to the origin) is then

$$t_c(a) = \begin{cases} \frac{1}{4}, & \text{if } \left| \frac{a-1}{a^2} \right| \geq \frac{1}{4} \text{ or } |a-1| < 1; \\ \frac{a-1}{a^2}, & \text{if } \left| \frac{a-1}{a^2} \right| < \frac{1}{4} \text{ and } |a-1| \geq 1. \end{cases} \quad (5)$$

Note that when a is real and positive, $\mathcal{D}(a) = -\log t_c(a)$, as given by (3) and (5). This then answers the question as to the generalisation of $\mathcal{D}(a)$ to complex a : we should use $-\log t_c(a)$, which is exactly the analytic continuation of the two branches of (3) which gives a continuous function in \mathbb{C} .

The curve in \mathbb{C} which delineates the two regions given in (5) is a branch of the curve

$$\left| \frac{a-1}{a^2} \right| = \frac{1}{4}. \quad (6)$$

The curve defined by (6) is a *limaçon*; it can be parametrised by $a = x + yi$, where

$$x = 2 + (2\sqrt{2} - 4 \cos \phi) \cos \phi \quad \text{and} \quad y = (2\sqrt{2} - 4 \cos \phi) \sin \phi \quad (7)$$

for $\phi \in [0, 2\pi)$. The limaçon has two “lobes”: taking only $\phi \in [\frac{\pi}{4}, \frac{7\pi}{4})$ gives the outer lobe, while $\phi \in [0, \frac{\pi}{4}) \cup (\frac{7\pi}{4}, 2\pi)$ gives the inner lobe (see Figure 2). The inner lobe lies entirely within the region $|a-1| \leq 1$, where the simple pole does not exist, so that the dominant singularity is still at $t = \frac{1}{4}$ there. As a result, it is precisely the outer lobe of the limaçon which separates the two regions defined by (5); as a crosses from one side of this curve to the other, $t_c(a)$ switches from one value to the other, and hence so too does $\mathcal{D}(a)$. We will use \mathcal{L}_O to denote the outer lobe of the limaçon and \mathcal{L}_I to denote the inner lobe.

3. Complex zeros are dense on the limaçon in the limit $n \rightarrow \infty$

In this section we will see that the curve \mathcal{L}_O not only divides the complex a -plane into two regions according to the asymptotic behaviour of $t_c(a)$ and $\mathcal{D}(a)$; it is also the case that all non-trivial roots of $D_{2n}(a)$ approach \mathcal{L}_O as $n \rightarrow \infty$, and that the roots become dense on \mathcal{L}_O in the limit. In this section we will assume that $a \neq 0$ or 2.

The two singularities in $D(t, a)$ (in equation (4)) contribute to the exponential growth of $D_{2n}(a)$. Expanding $D(t, a)$ around the point $t = \frac{1}{4}$ gives

$$D(t, a) = \frac{2}{2-a} \sum_{j=0}^{\infty} \left(\frac{a}{a-2} \right)^j (1-4t)^{j/2}. \quad (8)$$

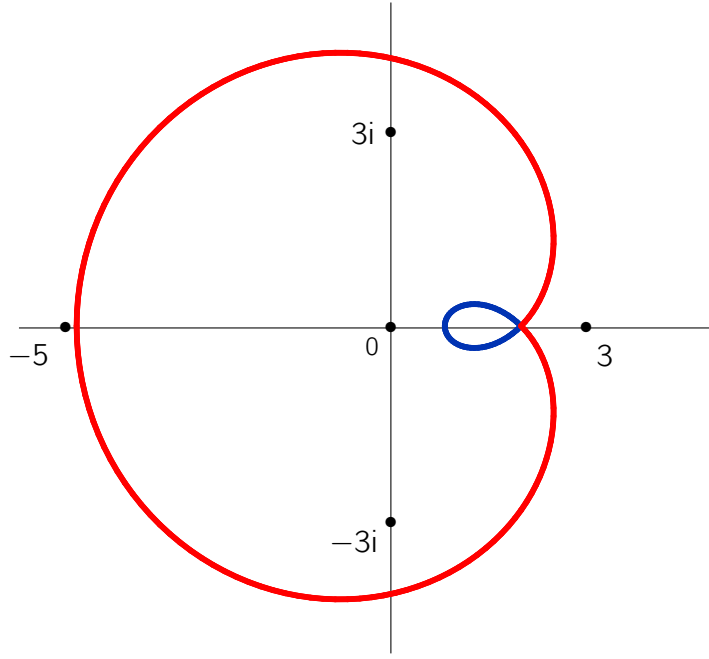


Figure 2: The limaçon defined by equation (6) has two lobes. The inner lobe lies inside the region $|a - 1| \leq 1$ and plays no role in the zeros of $D_{2n}(a)$. The outer lobe separates the two regions defined by equation (5): the dominant singularity is at $t = \frac{1}{4}$ when a is inside, and $t = \frac{a-1}{a^2}$ when a is outside.

This series becomes singular if $a \rightarrow 2$. To avoid this, bound a away from 2 by fixing $\delta > 0$ and defining

$$S_\delta = \{z \in \mathbb{C} \mid |z - 2| \geq \delta\}. \quad (9)$$

In what follows, assume that $a \in S_\delta$. Later in Section 5 we will address the case $a \rightarrow 2$.

By the Cauchy integral theorem, the terms in equation (8) contribute to the exponential growth of $D_{2n}(a)$. Computing the coefficients of t^n in equation (8) shows that $D_{2n}(a)$ can be cast in the form

$$r_n(a) = \frac{a}{(a-2)^2} \cdot \frac{4^n}{\sqrt{\pi n^3}} \sum_{\ell=0}^{\infty} \frac{g_\ell(a)}{n^\ell}. \quad (10)$$

This is done by expanding the factor

$$(1 - 4t)^{j/2} = \sum_{\ell=0}^{\infty} \left(-\frac{j}{2}\right)_\ell \frac{(4t)^\ell}{\ell!} \quad (11)$$

where $(a)_n$ is the Pochhammer function, and then determining the functions $g_\ell(a)$ term-by-term. Notice that $D_{2n}(a) = r_n(a)$ if $|a - 1| < 1$. The functions $g_\ell(a)$ are rational functions of a of the form

$$g_\ell(a) = \frac{q_\ell(a)}{(a-2)^\ell} \quad (12)$$

and $q_\ell(a)$ are computable polynomials of degree at most $\ell - 1$ in a . The sum in equation (10) can be rewritten to give

$$r_n(a) = \frac{a}{(a-2)^2} \cdot \frac{4^n}{\sqrt{\pi n^3}} \left(\sum_{\ell=0}^L \frac{g_\ell(a)}{n^\ell} + \frac{\beta_{L+1,n}(a)}{n^{L+1}} \right) \quad (13)$$

for any $L \geq -1$ (if $L = -1$ then the sum is empty), where (as long as $a \in S_\delta$) $\beta_{L+1,n}(a) \rightarrow g_{L+1}(a)$ as $n \rightarrow \infty$. That is, the sum in equation (10) can be truncated at any $\ell \geq 0$ and what remains will be a valid asymptotic expansion for the contribution of equation (8).

Expanding $D(t, a)$ in equation (4) near the simple pole gives

$$D(t, a) = \frac{a-2}{a-1} (1-At)^{-1} + \sum_{k=0}^{\infty} \frac{(-1)^k (a-1)^k}{(a-2)^{2k+1}} C_k (1-At)^k \quad (14)$$

where C_k are Catalan numbers and $A = \frac{a^2}{a-2}$. Determining the coefficients $p_n(a)$ of t^n gives, when $|a-1| \geq 1$,

$$p_n(a) = \frac{a-2}{a-1} \left(\frac{a^2}{a-1} \right)^n. \quad (15)$$

See also, for example, equation (5.17) in reference [13].

Lemma 1. *Let $\epsilon > 0$ and define $B_\epsilon = \{z \in \mathbb{C} \mid |z-1| \leq 1-\epsilon\}$. Then for all n sufficiently large, there are no zeros of $D_{2n}(a)$ inside B_ϵ .*

Proof. If $a \in B_\epsilon$ then the only singularity of $D(t, a)$ is the square root singularity at $t = \frac{1}{4}$. Thus $D_{2n}(a) = r_n(a)$ as per (10) or (13). Since $g_0(a) = 1$, truncate the sum to obtain the asymptotic form

$$r_n(a) \sim r_n^0(a) = \frac{a}{(a-2)^2} \cdot \frac{4^n}{\sqrt{\pi n^3}}. \quad (16)$$

For $a \in B_\epsilon$, $D_{2n}(a)$ can be made arbitrarily close to $r_n^0(a)$ by taking n sufficiently large (since $r_n^0(a)/r_n(a) \rightarrow 1$ as $n \rightarrow \infty$). But clearly $r_n(a) \neq 0$ for $a \in B_\epsilon$, so $D_{2n}(a)$ cannot have a zero there. \square

Outside of B_ϵ things are more interesting.

Lemma 2. *For each $n \geq 1$, let α_n be any sequence of non-trivial zeros of $D_{2n}(a)$ in S_δ . Then*

$$\left| \frac{\alpha_n^2}{\alpha_n - 1} \right| \rightarrow 4 \quad \text{as} \quad n \rightarrow \infty. \quad (17)$$

Proof. If $|a-1| < 1$ then $D_{2n}(a) = r_n(a)$, and by Lemma 1 there are no possible zeros for large n . Thus, assume that $|a-1| \geq 1$ so that $D_{2n}(a) = r_n(a) + p_n(a)$. If α_n is a zero of $D_{2n}(a)$, then we must have $|r_n(\alpha_n)| = |p_n(\alpha_n)|$. In this case $|r_n(\alpha_n)|$ grows at the exponential rate 4^n and $|p_n(\alpha_n)|$ grows at the exponential rate $\left| \frac{\alpha_n^2}{\alpha_n - 1} \right|^n$. If n is large then for α_n to be a zero it must (approximately) balance the two exponential growth rates for finite values of n . As $n \rightarrow \infty$ then the two growth rates must become equal. This can only happen if α_n satisfies equation (17).

Note that at first glance it may appear that $\alpha_n \rightarrow 0$ is also a valid possibility, but a more careful analysis shows that in that case $p_n(\alpha_n)$ would approach 0 exponentially faster than $r_n(\alpha_n)$. \square

Lemmas 1 and 2 immediately lead to the following.

Corollary 3. *As $n \rightarrow \infty$, all non-trivial zeros of $D_{2n}(a)$ approach the curve \mathcal{L}_O .*

Corollary 3 only establishes that as n gets large, all zeros of $D_{2n}(a)$ will be *somewhere* near \mathcal{L}_O . We also wish to show the converse of this result – that every point on \mathcal{L}_O is an accumulation point of zeros of $D_{2n}(a)$, so that the zeros become dense on \mathcal{L}_O as $n \rightarrow \infty$. We will prove the following.

Theorem 4. *Let $\epsilon, \delta > 0$. Then for every every n sufficiently large and for every point $a^* \in \mathcal{L}_O \cap S_\delta$, there is a zero of $D_{2n}(a)$ in the region $|a - a^*| \leq \epsilon$.*

To show this, we will estimate the locations of the zeros by using an approach similar to that used in reference [1], where it was shown that poles of a certain generating function become dense on parts of the unit circle.

Define the approximation

$$D_{2n}^0(a) = p_n(a) + r_n^0(a) = \frac{a-2}{a-1} \left(\frac{a^2}{a-1} \right)^n + \frac{a}{(a-2)^2} \frac{4^n}{\sqrt{\pi n^3}}. \quad (18)$$

For $|a - 1| \geq 1$, $D_{2n}^0(a)$ is an asymptotic approximation for $D_{2n}(a)$; that is, $D_{2n}^0(a)/D_{2n}(a) \rightarrow 1$ as $n \rightarrow \infty$. It follows that, in this region, the zeros of $D_{2n}^0(a)$ give asymptotic approximations to the zeros of $D_{2n}(a)$. Note that $D_{2n}^0(a)$ is not a good approximation in the region $|a - 1| < 1$; as we will see later, $D_{2n}^0(a)$ has zeros inside this region which collect on the inner lobe \mathcal{L}_I , while $D_{2n}(a)$ does not.

The form (6) of the limaçon suggests that a change of variables will be convenient. Define $A = \frac{a^2}{a-1}$ and solve for a in terms of A :

$$a = a^+ \equiv a^+(A) = \frac{1}{2}(A + \sqrt{A} \sqrt{A-4}). \quad (19)$$

When $|A| = 4$, the solution a^+ is on \mathcal{L}_O . (The other solution to the quadratic gives a point on \mathcal{L}_I .) Setting

$$f(a) = \frac{a-2}{a-1} \quad \text{and} \quad g(a) = \frac{a}{(a-2)^2},$$

we then have

$$D_{2n}^0(a^+) = f(a^+)A^n + g(a^+) \frac{4^n}{\sqrt{\pi n^3}}. \quad (20)$$

Proof of Theorem 4. Assume that the complex A -plane has a branch cut along the positive real axis. Fix integers p and q so that $\theta = \frac{p}{q}\pi \in (0, 2\pi)$ and $a^+(4e^{i\theta}) \in S_\delta$. Set $n = 2kq$. We will show that $4e^{i\theta}$ is an accumulation point for roots of $D_{2n}^0(a^+)$ in the A -plane. This in turn means that $a^+(4e^{i\theta})$ is an accumulation point for roots of $D_{2n}^0(a)$, and since $D_{2n}^0(a)$ is an asymptotic approximation for $D_{2n}(a)$, the result will follow.

Set $A_n = 4e^{i\theta}(1 + s_n)$ for an as-yet (small) unknown s_n and write $a_n^+ = a^+(A_n)$. Then substitute $A = A_n$ in (20). To leading order, this gives

$$D_{2n}^0(a_n^+) = F(4e^{i\theta})(4^n(1 + s_n)^n)(1 + O(s_n)) + G(4e^{i\theta}) \frac{4^n}{\sqrt{\pi n^3}} (1 + O(s_n)) \quad (21)$$

where $F(A) = f(a_+)$ and $G(A) = g(a_+)$. (This uses the analyticity of f and g away from $a = 2$.)

Notice that $F(4e^{i\theta})$ is nonzero except when $\theta = 0$ (this is excluded), and that $G(4e^{i\theta})$ is nonzero. Equation (21) thus shows that there is a zero of (20) close to $A = 4e^{i\theta}$ for our chosen θ . This solution is well approximated by ignoring the $O(s_n)$ terms, approximating $1 + s_n = e^{s_n + O(s_n^2)}$, and solving for s_n in (21). This gives the following approximation for s_n :

$$s_n \sim \frac{1}{n} \log \left(\frac{-1}{\sqrt{\pi n^3}} \frac{G(4e^{i\theta})}{F(4e^{i\theta})} \right) = \frac{1}{n} \log \left(\frac{-1}{\sqrt{\pi n^3}} \frac{e^{i\theta/2}}{4(e^{i\theta} - 1)^{3/2}} \right). \quad (22)$$

This shows that $s_n \rightarrow 0$ as $n \rightarrow \infty$, and hence $a_n^+ \rightarrow 4e^{i\theta}$. Since θ was an arbitrary rational multiple of π and the circle $|A| = 4$ maps continuously to \mathcal{L}_O in the a -plane, it follows that for $a^* \in \mathcal{L}_O \cap S_\delta$ there is a choice of θ and an n sufficiently large so that there is a root of $D_{2n}^0(a)$ within the region $|a - a^*| \leq \epsilon$. Then since $D_{2n}^0(a) \rightarrow D_{2n}(a)$, the result of the theorem follows. \square

Note that more precise approximations for s_n can be obtained by replacing $r_n^0(a)$ in equation (18) with higher-order truncations of $r_n(a)$, for example

$$r_n^1(a) = \frac{a}{(a-2)^2} \cdot \frac{4^n}{\sqrt{\pi n^3}} \left(1 - \frac{3a^2}{2(a-2)^2 n} \right). \quad (23)$$

This changes the form of $g(a)$ and $G(A)$, but since all the $g_\ell(a)$ have a form given by (12), the analyticity away from $a = 2$ still holds and all of the above steps will still be valid.

4. Numerical approximation of the zeros

The method used to prove Theorem 4 gives an approximation for the zero of $D_{2n}(a)$ closest to any point in $\mathcal{L}_O \cap S_\delta$. However, this does not give much insight as to how the zeros “move” as n changes. For example, the non-trivial zeros of $D_{2n}(a)$ can be ordered according to their argument, and then for some given k (either constant or depending on n) the behaviour of the k -th zero can be investigated. In this section and the next, we will pursue this question, using two different methods – one which works well away from $a = 2$, and another which specifically probes the $a \rightarrow 2$ regime.

We continue to assume $|a - 1| \geq 1$, so that $D_{2n}(a) = p_n(a) + r_n(a)$. If a is a zero of $D_{2n}(a)$ then we can write, using equations (10) and (15)

$$\left(\frac{a^2}{a-1} \right)^n = - \left(\frac{4^n}{\sqrt{\pi n^3}} \right) \left(\frac{a(a-1)}{(a-2)^3} + \frac{(a-1)\beta_{1,n}(a)}{n(a-2)} \right). \quad (24)$$

This may be put in the form

$$a^2 = 4(a-1)e^{(2k+1)\pi i/n} \left(\frac{1}{\sqrt{\pi n^3}} \right)^{1/n} \left(\frac{a(a-1)}{(a-2)^3} + \frac{(a-1)\beta_{1,n}(a)}{n(a-2)} \right)^{1/n} \quad (25)$$

for $k = 0, 1, 2, \dots, n-1$.

We will now attempt to compute approximate solutions to (25) by replacing $\beta_{1,n}(a)$ with a *constant* β . Note that if $\beta = 0$ then we are finding roots of $D_{2n}^0(a)$ as per equation

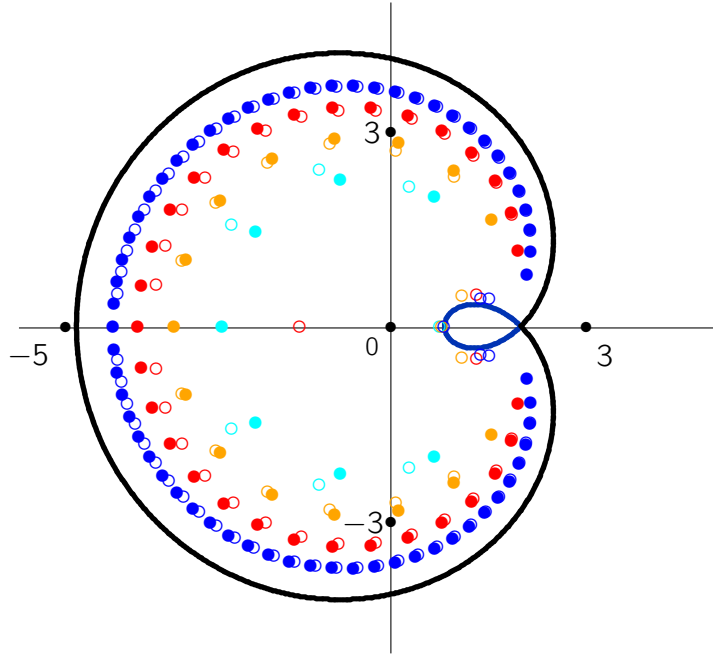


Figure 3: Approximate (○) and exact zeros (●) for $n \in \{8, 16, 32, 64\}$. The approximate solutions are obtained by solving equation (25) with $\beta = 4$.

(18). In Figure 3 the solutions for $n \in \{16, 32, 48\}$ are shown with $\beta = 4$ (open circles). The exact solutions are shown by the bullets for these values of n , and the limaçon in Figure 2 is the closed curve.

In Figure 4 the effects of β on the location of approximate zeros are examined. The exact zeros for $n = 16$ and $n = 32$ are plotted (denoted by bullets). Approximations for $\beta \in \{\pm 4, \pm 4i\}$ are shown as open circles. For $n = 32$ the estimates cluster close to the exact values. This is less so for $n = 16$, but even in this case the effects of β are damped down in equation (25). Thus, we will restrict our attention to the case $\beta = 0$, and work on finding approximate solutions to $D_{2n}^0(a) = 0$.

Put $\beta = 0$ in equation (25) to obtain

$$a^2 = 4(a-1)e^{(2k+1)\pi i/n} \left(\frac{1}{\sqrt{\pi n^3}} \right)^{1/n} \left(\frac{a(a-1)}{(a-2)^3} \right)^{1/n}. \quad (26)$$

Define the functions

$$\sigma_{k,n} = e^{(2k+1)\pi i/n}, \quad h_n = \left(\frac{1}{\sqrt{\pi n^3}} \right)^{1/n}, \quad H_n(a) = \left(\frac{a(a-1)}{(a-2)^3} \right)^{1/n}. \quad (27)$$

Use these definitions to write equation (26) in the following form:

$$a^2 = 4(a-1)\sigma_{k,n} h_n H_n(a). \quad (28)$$

If it was the case that $H_n(a)$ did not depend on a , then this equation can be solved for a . Thus, our strategy is to find an approximation for a so that $H_n(a)$ can be approximated as a function of (k, n) , and then to solve the resulting equation for a . Since $H_n(a) \rightarrow 1$ as $n \rightarrow \infty$, replace it by 1 in equation (28) to find the reduced equation

$$a^2 = 4(a-1)\sigma_{k,n} h_n \quad (29)$$

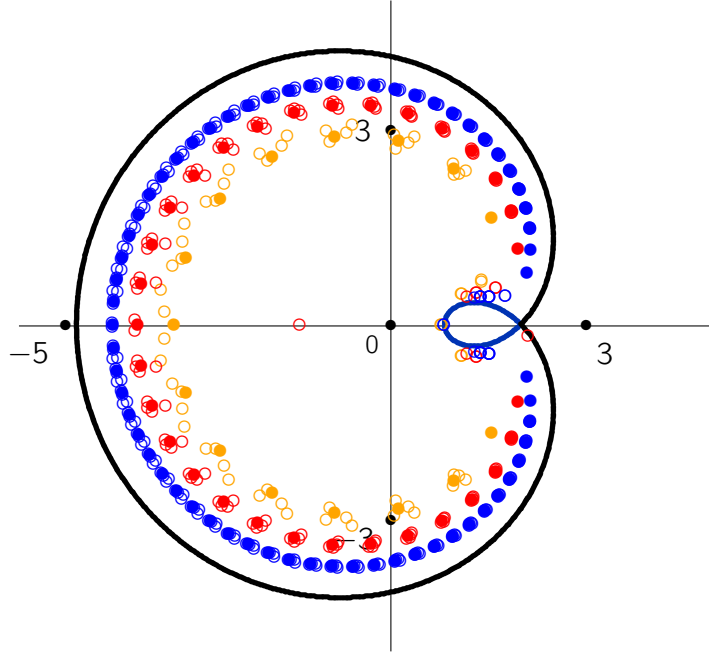


Figure 4: Approximate (o) and exact zeros (•) for $n = 16$, $n = 32$ and $n = 64$ and for $\beta \in \{\pm 4, \pm 4i\}$. For $n = 32$ and $n = 64$ the zeros and estimated zeros cluster together, but less so for $n = 16$. Notice that the numerical procedure finds, in some cases, solutions on the other branch of the limaçon.

for approximate zeros. The solutions of this equation are

$$a'_\pm = 2\sigma_{k,n}h_n \pm 2\sqrt{\sigma_{k,n}h_n} \sqrt{\sigma_{k,n}h_n - 1}. \quad (30)$$

Substituting this in $H_n(a)$ in equation (28) gives the following asymptotic expression for $H_n(a_0)$:

$$H_n(a'_\pm) \sim 1 + \frac{1}{n} \log \left(\frac{(\sigma_{k,n} \pm \sqrt{\sigma_{k,n}} \sqrt{\sigma_{k,n} - 1})(2\sigma_{k,n} \pm 2\sqrt{\sigma_{k,n}} \sqrt{\sigma_{k,n} - 1} - 1)}{4(\sigma_{k,n} - 1 \pm \sqrt{\sigma_{k,n}} \sqrt{(\sigma_{k,n} - 1)})^3} \right). \quad (31)$$

Proceed by substituting $H_n(a)$ in equation (28) with this asymptotic expression, and denote the solutions by a'' . There are two choices of the sign in equation (31), and in total four solutions are found. However, these are in identical pairs so that only two distinct solutions are obtained. Asymptotic expansions of these two solutions are

$$\begin{aligned} a''_\pm &\simeq 2\sigma_{k,n} \pm 2\sqrt{\sigma_{k,n}} \sqrt{\sigma_{k,n} - 1} \\ &\mp \frac{1}{n} \left(\frac{3}{2} \log n + 2 \log 2 + \frac{1}{2} \log \pi \right) \frac{\sqrt{\sigma_{k,n}} (2\sigma_{k,n} \pm 2\sqrt{\sigma_{k,n}} \sqrt{\sigma_{k,n} - 1} - 1)}{\sqrt{\sigma_{k,n} - 1}} \\ &\pm \frac{1}{n} \frac{\sqrt{\sigma_{k,n}} (2\sigma_{k,n} \pm 2\sqrt{\sigma_{k,n}} \sqrt{\sigma_{k,n} - 1} - 1)}{\sqrt{\sigma_{k,n} - 1}} \times \\ &\log \left(\frac{(\sigma_{k,n} + \sqrt{\sigma_{k,n}} \sqrt{\sigma_{k,n} - 1})(2\sigma_{k,n} + 2\sqrt{\sigma_{k,n}} \sqrt{\sigma_{k,n} - 1} - 1)}{(\sigma_{k,n} + \sqrt{\sigma_{k,n}} \sqrt{\sigma_{k,n} - 1} - 1)^3} \right). \end{aligned} \quad (32)$$

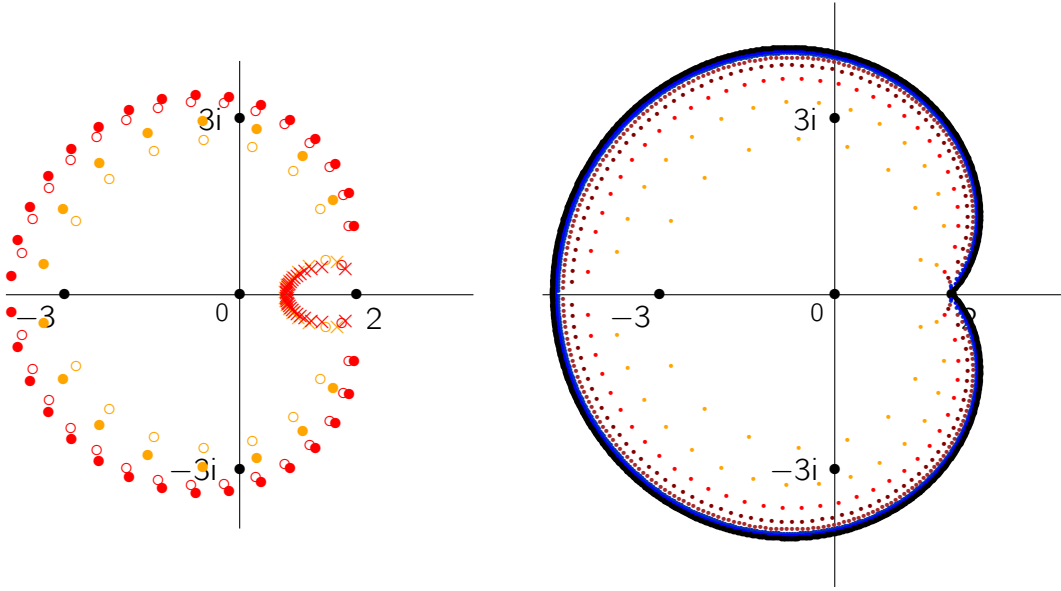


Figure 5: Left panel: Approximate zeros computed from equation (32). The a''_+ are denoted by \circ , the a''_- are denoted by \times , and exact zeros by \bullet . The data are for $N = 16$ and $n = 32$. Notice that the a''_- are located on the other branch of the limaçon while the a''_+ are approximate zeros on the first branch. Right panel: The zeros a''_+ for $n \in \{16, 32, 64, 128, 256, 512, 1024\}$. For larger values of n the zeros approach the limaçon which is plotted around the zeros.

In the left panel in Figure 5 the a''_\pm are plotted for $n = 16$ and $n = 32$. The bullets are exact locations of partition function zeros, and the estimates a''_\pm are shown by open circles (for a''_+) and crosses (for a''_-). This shows that the choice of the $+$ -sign in equation (32) gives approximations to the partition function zeros, while the a''_- are points located close to the other branch \mathcal{L}_1 of the limaçon. Notice in particular that equation (32) does not produce approximation to all the zeros – there are two zeros for each value of n near the negative real axis which are not approximated. In addition, there are two extra approximations for each value of n near the positive real axis. The remaining zeros are approximated well.

In the right panel of Figure 5, the approximate zeros a''_+ are plotted for $n \in \{16, 32, 64, 128, 256, 512, 1024\}$. With increasing n these approach the limaçon. Putting $k = \lfloor \rho n \rfloor$ in equation (32) and then taking $n \rightarrow \infty$ gives

$$a''(\rho) = \lim_{n \rightarrow \infty} a''_+ = 2e^{2\rho\pi i} + 2e^{\rho\pi i} \sqrt{e^{2\rho\pi i} - 1} \quad (33)$$

which is an alternative parametrization of the limaçon given by equation (6).

5. Asymptotics for the leading zero

Numerical exploration shows that the choice $k = 1$ in equation (32) is a very good approximation to the leading zero a_0^\dagger (that is, of the zero of $D_{2n}(a)$ with smallest positive principal argument). The choice $k = 2$ seems to approximate the next to leading zero as n increases, but the choice $k = 0$ is a spurious zero, which has no counterpart amongst

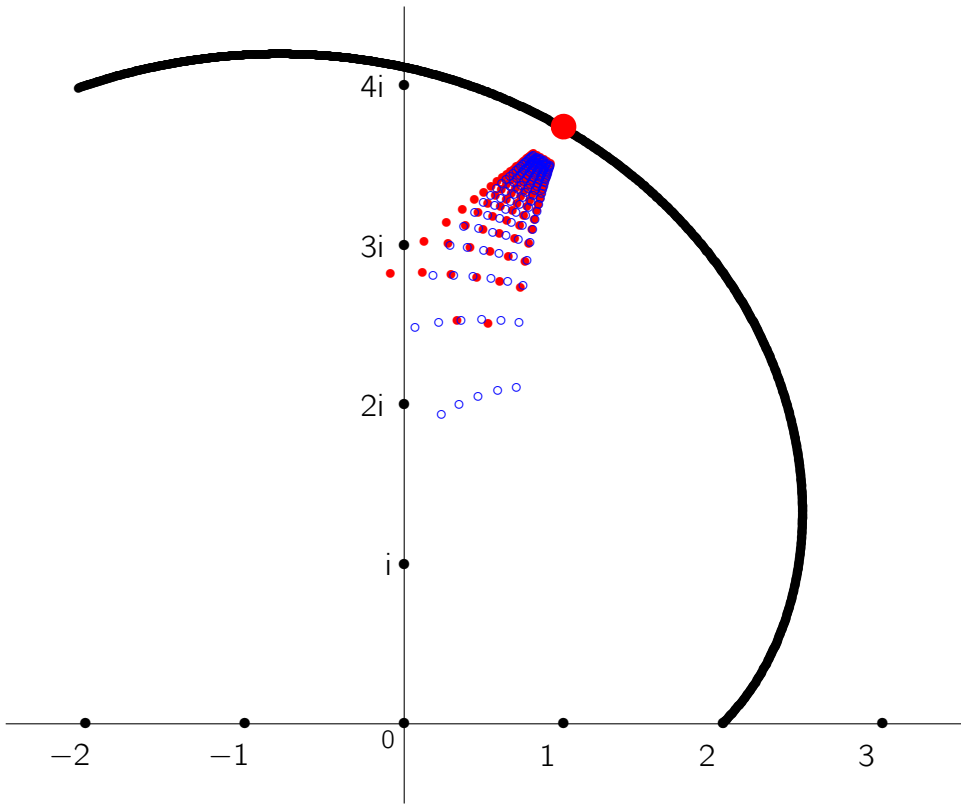


Figure 6: Exact zeros (denoted by \bullet 's) converging to the point with argument equal to $\frac{5}{12}\pi$ on the limaçon (determined by putting $\rho = \frac{1}{6}$ in equation (33)). Approximate zeros (denoted by \circ 's) were computed from equation (32). The exact zeros were computed for $10 \leq n \leq 150$ from $D_{2n}(a)$.

the zeros of $D_{2n}(a)$.

There are two short-comings about equation (32). The first is that the approximations leading to it introduced a few new zeros, and the second is that, since all zeros approaches 2 as $n \rightarrow \infty$ for fixed k , the approximations a''_+ must leave the set S_δ on which the approximation was done. This, for example, show that equation (32) is not an approximation to the k -th zero for fixed k , since the k -th zero converges to 2 and so leaves the set S_δ . On the other hand, if $k = \lfloor \rho n \rfloor$, and $n \rightarrow \infty$, then equation (32) is an approximation for the zeros. This is, for example, shown in figure 6 for the choice $\rho = \frac{1}{6}$, which corresponds to the point with argument $\frac{5}{12}\pi$ on the limaçon. Exact zeros and approximate zeros computed from equation (32) both converge to the limiting point.

In order to find asymptotic approximations of the location of the leading zero, we will approximate the partition function $D_{2n}(a)$ (see equation (1)). The leading zero approaches 2 at a rate proportional to $1/\sqrt{n}$, so, to first order, $a_1 = 2 + O(1/\sqrt{n})$. That is, we will consider $D_{2n}(2 + \frac{c}{\sqrt{n}})$ and determine c . Notice that

$$D_{2n}(2 + \frac{c}{\sqrt{n}}) = \sum_{k=0}^n \sum_{\ell=k}^n \frac{2\ell+1}{n+\ell+1} \binom{2n}{n+\ell} \binom{\ell}{k} \frac{c^k}{n^{k/2}}. \quad (34)$$

For fixed n the summand is maximized when

$$k \simeq \frac{c^2 n}{(\sqrt{n} + c)(2\sqrt{n} + c)} = \frac{1}{2} c^2 - \frac{3}{4} \frac{c^3}{\sqrt{n}} + O\left(\frac{1}{n}\right); \quad (35)$$

$$\ell \simeq \frac{c n}{2\sqrt{n} + c} = \frac{1}{2} c \sqrt{n} - \frac{1}{4} c^2 + O\left(\frac{1}{\sqrt{n}}\right). \quad (36)$$

Putting $n = m^2$ and $\ell = \lambda m$ and using Stirling's approximation to approximate factorials in the binomial coefficients in the summand in equation (34) gives

$$\frac{2\ell + 1}{n + \ell + 1} \binom{2n}{n + \ell} \binom{\ell}{k} \frac{c^k}{n^{k/2}} \simeq \frac{2^{2m^2+1} e^{-\lambda^2} c^k \lambda^{k+1}}{\sqrt{\pi} m^2 k!} (1 + o(1)) \quad (37)$$

to leading order. The summation over ℓ can be approximated by integrating this over λ (using $\frac{d\ell}{d\lambda} = m$):

$$\sum_{\ell=k}^n \frac{2\ell + 1}{n + \ell + 1} \binom{2n}{n + \ell} \binom{\ell}{k} \frac{c^k}{n^{k/2}} \sim \int_0^\infty \frac{2^{2m^2+2} e^{-\lambda^2} c^k \lambda^{k+1}}{\sqrt{\pi} m^2 k!} m d\lambda \quad (38)$$

$$= \frac{2^{2m^2-k} c^k}{m \Gamma(\frac{1}{2}(k+1))}. \quad (39)$$

Summing over k then gives the asymptotic formula

$$D_{2n}(2 + \frac{c}{\sqrt{n}}) \sim \frac{4^n}{2\sqrt{\pi n}} \left(2 + c\sqrt{\pi} e^{c^2/4} (1 + \operatorname{erf}(\frac{c}{2})) \right). \quad (40)$$

The *error function* is defined by

$$\operatorname{erf}(x) = \frac{2}{\sqrt{\pi}} \int_0^x e^{-t^2} dt \quad (41)$$

for real x , and can be analytically continued to the entire complex plane. If $c = 0$ then $D_{2n}(2) \sim \frac{1}{\sqrt{\pi n}} 4^n$, which is the correct asymptotics at $a = 2$.

Zeros of $D_{2n}(a)$ are found at solutions of

$$F(c) = 2 + c\sqrt{\pi} e^{c^2/4} (1 + \operatorname{erf}(\frac{c}{2})) = 0. \quad (42)$$

The leading zero will correspond to that solution c with smallest principal argument. Solving numerically gives

$$c = 2.450314191845586\dots + 5.094256056412729\dots \times i \quad (43)$$

and this shows that the leading root approaches the critical point $a = 2$ along

$$a_1 = 2 + \frac{2.450314191845586\dots}{\sqrt{n}} + \frac{5.094256056412729\dots \times i}{\sqrt{n}} + O\left(\frac{1}{n}\right). \quad (44)$$

Asymptotics for the next to leading zero can be determined by finding the appropriate solution of equation (42). The result is

$$a_2 = 2 + \frac{4.051192261300444\dots}{\sqrt{n}} + \frac{6.323878106240248\dots \times i}{\sqrt{n}} + O\left(\frac{1}{n}\right). \quad (45)$$

The next term in equations (44) and (45) can be determined by computing the next term in equation (37). This is

$$4^{m^2} \left(\frac{2 e^{-\lambda^2} c^k \lambda^{k+1}}{\sqrt{\pi} m^2 k!} + \frac{e^{-\lambda^2} (1 + k + k^2 - 2\lambda^2) c^k \lambda^k}{\sqrt{\pi} m^3 k!} + O\left(\frac{1}{m^4}\right) \right). \quad (46)$$

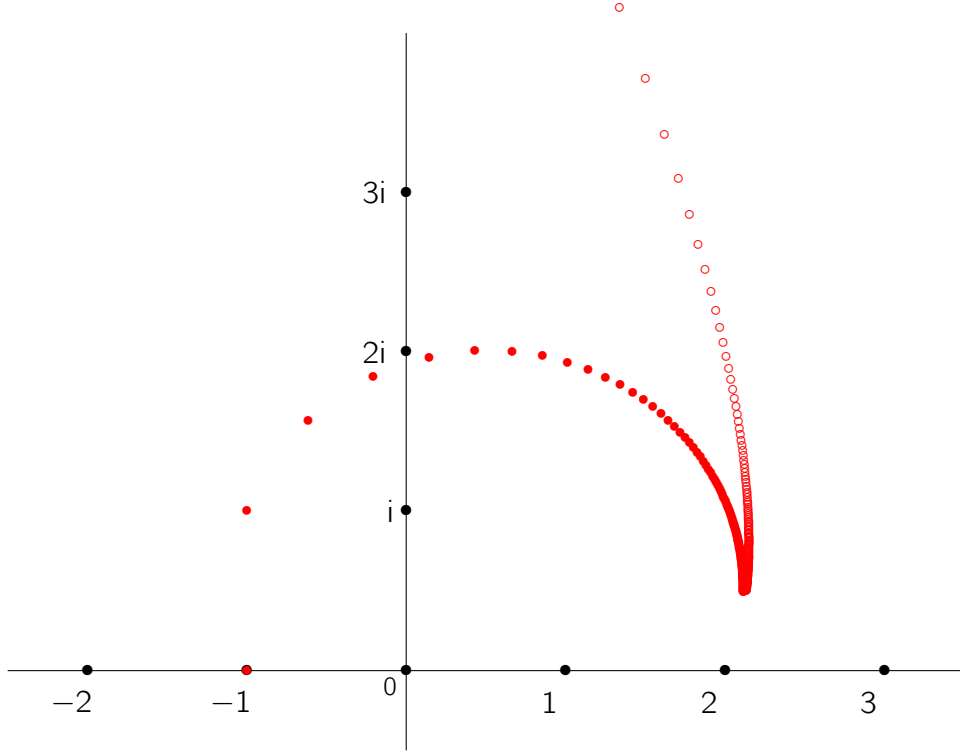


Figure 7: Leading zeros (denoted by \bullet 's) and the asymptotic approximations to leading zeros (denoted by \circ 's). The approximation to leading zeros is given by a_1 in equation (49). The approximation is poor for small values of n , but improves quickly with increasing values of n .

Computing an improved asymptotic formula for the partition from this gives

$$D_{2n}(2 + \frac{c}{\sqrt{n}}) \sim \frac{4^n}{2\sqrt{\pi n}} \left(2 + c\sqrt{\pi} e^{c^2/4} (1 + \text{erf}(\frac{c}{2})) - \frac{c}{4\sqrt{n}} \left(2(2 + c^2) + \sqrt{\pi} c(4 + c^2)(1 + \text{erf}(\frac{c}{2})) e^{c^2/4} \right) \right). \quad (47)$$

Put $c = c_1 + c_2 \frac{1}{\sqrt{n}}$ in the above, and set c_1 to be the value in equation (43), so as to eliminate the $\frac{1}{\sqrt{n}}$ term in (47). The $\frac{1}{n}$ term in equation (47) is then eliminated by putting

$$c_2 = -9.97370256476894\dots + 12.482527911923\dots \times i. \quad (48)$$

This improves the asymptotic for the leading zero a_1 in equation (44) to

$$a_1 = 2 + \frac{c_1}{\sqrt{n}} + \frac{c_2}{n} + O\left(\frac{1}{\sqrt{n^3}}\right). \quad (49)$$

In figure 7 the exact leading zero for $n \leq 150$ is shown by bullets while the open circles are computed from equation (49). The approximation is poor for small values of n , but improves when n increases and the zeros approaches the point $a = 2$.

6. Conclusions

In this paper we have examined the zeros of the partition function $D_{2n}(a)$ of adsorbing Dyck paths of length $2n$. These zeros are distributed over a region of the complex plane,

but as n becomes large they all (except for a single root at $a = 0$) collect on a certain closed curve. We have shown that this curve is one lobe of a limaçon, and that as $n \rightarrow \infty$ the roots become dense on this curve (see theorem 4).

In addition, we determined a formula approximating the locations of zeros for finite values of n (equation (32)), and developed an asymptotic formula for the location of the leading zeros as $n \rightarrow \infty$ (see equation (49)). In the limit as $n \rightarrow \infty$ the leading zeros converge to the point $a_c = 2$, forming an edge-singularity on the positive real axis. The rate of convergence to the edge-singularity is given in equation (49) as $O(1/\sqrt{n})$, and this is consistent with the crossover exponent of adsorbing Dyck paths having value $\phi = \frac{1}{2}$ (see, for example, references [12, 13]).

Adsorbing Dyck paths are just one example of a solvable model of interacting polymers. Another closely related model is that of *pulled ballot paths*, which can be used to represent a linear polymer chain being pulled from a surface by an external force. In that case the curve on which the zeros accumulate turns out to be the outer boundary of two circles of radius $\sqrt{2}$, centred at $\pm i$. There are many other solvable models in statistical mechanics, and the zeros of other models may display a variety of behaviours.

Acknowledgements: EJJvR acknowledges financial support from NSERC (Canada) in the form of a Discovery Grant. NRB is supported by the Australian Research Council grant DE170100186.

References

- [1] M Bousquet-Mélou. Families of prudent self-avoiding walks. *Journal of Combinatorial Theory, Series A*, 117(3):313–344, 2010.
- [2] R Brak, JW Essam, and AL Owczarek. New results for directed vesicles and chains near an attractive wall. *J Stat Phys*, 93:155–192, 1998.
- [3] JL Cardy. Conformal invariance and the Yang-Lee edge singularity in two dimensions. *Phys Rev Lett*, 54(13):1354–1356, 1985.
- [4] P-G de Gennes. *Scaling Concepts in Polymer Physics*. Cornell, 1979.
- [5] K De'Bell and T Lookman. Surface phase transitions in polymer systems. *Rev Mod Phys*, 65:87–113, 1993.
- [6] ME Fisher. Correlation functions and the critical region of simple fluids. *J Math Phys*, 5(7):944–962, 1964.
- [7] ME Fisher. Lectures in Theoretical Physics. Vol VII C (U Colorado Press 1965), 1965.
- [8] G Forgacs, V Privman, and HL Frisch. Adsorption–desorption transition of polymer chains interacting with surfaces. *J Chem Phys*, 90:3339–3345, 1989.
- [9] JM Hammersley, GM Torrie, and SG Whittington. Self-avoiding walks interacting with a surface. *J Phys A: Math Gen*, 15:539–571, 1982.
- [10] F Hanke, L Livadaru, and HJ Kreuzer. Adsorption forces on a single polymer molecule in contact with a solid surface. *EPL (Europhysics Letters)*, 69(2):242–248, 2004.
- [11] H Haschke, MJ Miles, and V Koutsos. Conformation of a single polyacrylamide molecule adsorbed onto a mica surface studied with atomic force microscopy. *Macromolecules*, 37(10):3799–3803, 2004.
- [12] EJ Janse van Rensburg. The adsorption transition in directed paths. *J Stat Mech: Theo Expr*, 2010:P08030, 2010.
- [13] EJ Janse van Rensburg. *The Statistical Mechanics of Interacting Walks, Polygons, Animals and Vesicles*. Oxford University Press, 2 edition, 2015.

- [14] EJ Janse van Rensburg. Microcanonical simulations of adsorbing self-avoiding walks. *Journal of Statistical Mechanics: Theory and Experiment*, 2016(3):033202, 2016.
- [15] EJ Janse van Rensburg. Partition and generating function zeros in adsorbing self-avoiding walks. *Journal of Statistical Mechanics: Theory and Experiment*, 2017(3):033208, 2017.
- [16] EJ Janse van Rensburg and AR Rechnitzer. Multiple Markov chain Monte Carlo study of adsorbing self-avoiding walks in two and in three dimensions. *Journal of Physics A: Mathematical and General*, 37(27):6875–6898, 2004.
- [17] S-Y Kim and RJ Creswick. Yang-Lee zeros of the q -state Potts model in the complex magnetic field plane. *Phys Rev Lett*, 81(10):2000–2003, 1998.
- [18] S-Y Kim and RJ Creswick. Density of states, Potts zeros, and Fisher zeros of the q -state Potts model for continuous q . *Phys Rev E*, 63(6):066107, 2001.
- [19] DA Kurtze and ME Fisher. Yang-Lee edge singularities at high temperatures. *Phys Rev B*, 20(7):2785–2796, 1979.
- [20] T-D Lee and C-N Yang. Statistical theory of equations of state and phase transitions. II Lattice gas and Ising model. *Phys Rev*, 87(3):410–419, 1952.
- [21] V Privman, G Forgacs, and HL Frisch. New solvable model of polymer-chain adsorption at a surface. *Physical Review B*, 37(16):9897–9900, 1988.
- [22] D Ruelle. *Statistical Mechanics*. Addison-Wesley, 4 edition, 1983.
- [23] T Vrbová and SG Whittington. Adsorption and collapse of self-avoiding walks in three dimensions: a Monte Carlo study. *J Phys A: Math Gen*, 31:3989–3998, 1998.
- [24] SG Whittington. A directed-walk model of copolymer adsorption. *Journal of Physics A: Mathematical and General*, 31(44):8797–8803, 1998.
- [25] C-N Yang and T-D Lee. Statistical theory of equations of state and phase transitions. I Theory of condensation. *Phys Rev*, 87(3):404–409, 1952.